International Journal of Thermophysics, Vol. 26, No. 5, September 2005 (© 2005)
DOI: 10.1007/s10765-005-8093-6

Self-Diffusion and Binary Maxwell–Stefan Diffusion Coefficients of Quadrupolar Real Fluids from Molecular Simulation

G. A. Fernández,[1] J. Vrabec,[1,2] and H. Hasse[1]

Received September 21, 2004

Self- and binary Maxwell–Stefan (MS) diffusion coefficients were determined by equilibrium molecular dynamics simulations with the Green–Kubo method. This study covers self-diffusion coefficients at liquid states for eight pure fluids, i.e., F_2, N_2, CO_2, CS_2, C_2H_6, C_2H_4, C_2H_2, and SF_6 as well as MS diffusion coefficients for three binary mixtures N_2+CO_2, N_2+C_2H_6, and CO_2+C_2H_6. The fluids were modeled by the two-center Lennard–Jones plus point-quadrupole pair potential, with parameters taken from previous work of our group which were determined solely on the basis of vapor–liquid equilibrium data. Self-diffusion coefficients are predicted with a statistical uncertainty less than 1%, and they agree within 2–28% with the experimental data. The correction of the simulation data due to the finite size of the system increases the value of the self-diffusion coefficient typically by 10%. If this correction is considered, better agreement with the experimental data can be expected for most of the studied fluids. MS diffusion coefficients for three binary mixtures were also predicted; their statistical uncertainty is about 10%. These results were used to test three empirical equations to estimate MS diffusion coefficients in binary mixtures, i.e., the equations of Caldwell and Babb, of Darken, and of Vignes. The equations of Caldwell and Babb and of Vignes show qualitatively different behavior of the MS diffusion coefficient than that observed in the simulations. In agreement with previous work, the best results are obtained in all cases with the equation of Darken.

KEY WORDS: binary diffusion; Green–Kubo method; Maxwell–Stefan; molecular dynamics; molecular simulation; self-diffusion; quadrupole; two-center Lennard–Jones potential.

[1] Institute of Thermodynamics and Thermal Process Engineering, University of Stuttgart, D-70550 Stuttgart, Germany.
[2] To whom correspondence should be addressed. E-mail: vrabec@itt.uni-stuttgart.de

1. INTRODUCTION

Traditionally, self-diffusion coefficients and Maxwell–Stefan diffusion coefficients in mixtures are obtained from empirical correlations or with more or less theoretically based equations. Although very successful in practical applications, this approach is limited to the range where correlations were adjusted to experimental data and, thus, by the availability of experimental data to fit such correlations. With increasing computer power, molecular simulation has become an interesting alternative tool to investigate a wide range of phenomena in many fields of science and engineering, among which is diffusion. The first simulation studies on self-diffusion coefficients date back to the 1960s, when Alder and Wainwright [1, 2] carried out simulations with hard spheres and discovered the long-time tail of the velocity correlation function. Furthermore, Jacucci and McDonald [3], Jolly and Bearman, and Schoen and Hoheisel [4, 5] carried out computations of the binary transport coefficients, and investigated the contribution of the cross correlation to the binary Maxell–Stefan (MS) diffusion coefficient. These studies established the calculation methodology and paved the way for subsequent studies aimed to predict diffusion coefficients. More recently and from an engineering point of view, Stoker and Rowley [6, 7] used molecular simulation to calculate binary MS diffusion coefficients of binary alkane mixtures. They proposed calculating binary MS diffusion coefficients from self-diffusion coefficient data.

In recent work of our group, it was shown that the Lennard–Jones (LJ) potential, adjusted only to experimental vapor–liquid equilibria, satisfactorily predicts the self- and binary MS diffusion coefficients [8], shear viscosities, and thermal conductivities [9] of several simple fluids and their mixtures. These results confirm the known suitability of the spherical LJ potential to describe these fluids [10], and also show that the determination of the potential parameters from vapor–liquid equilibria is an adequate choice to predict transport properties with reasonable accuracy, at least for simple fluids.

Here, this investigation is extended to more complex molecules. The intermolecular interactions are described by the two-center Lennard–Jones plus point-quadrupole (2CLJQ) potential. This model has been employed successfully by several authors, for modeling thermodynamic properties and the self-diffusion coefficients of simple real fluids [11–15]. Although the 2CLJQ potential is not new, the prediction of transport properties with such a model has still not been explored in detail. In order to investigate the suitability and performance of the 2CLJQ potential with respect to self-diffusion coefficients, they were calculated in the present work for a range of molecular fluids (F_2, N_2, CO_2, CS_2, C_2H_6, C_2H_4,

C_2H_2, SF_6) and compared to existing experimental data for these fluids. Good predictions of the self-diffusion coefficients were observed in most cases. Also self- and MS diffusion coefficients for the binary mixtures $N_2 + CO_2$, $N_2 + C_2H_6$, and $CO_2 + C_2H_6$ were studied. These results were used to evaluate the performance of three equations for describing binary MS diffusion coefficients, namely, the equations of Caldwell and Babb [16], Darken [17], and Vignes [18]. A direct comparison of simulation results to experimental data of binary MS diffusion coefficients is not possible for the fluids studied here, because of the lack of such data.

2. METHOD

2.1. Molecular Model

In the present work, interactions between molecules are described by 2CLJQ based potential models. These models have recently been developed in our group [15] as part of a study covering 25 pure substances. The 2CLJQ model is a pairwise additive potential model consisting of two Lennard–Jones sites a distance L apart plus a point-quadrupole of moment Q located in the geometric center of the molecule and oriented along the molecular axis, which connects the two LJ sites. The interaction energy of two molecules i and j is

$$u_{ij}^{2\mathrm{CLJQ}} = \sum_{a=1}^{2}\sum_{b=1}^{2} 4\epsilon_{ij}\left[\left(\frac{\sigma_{ij}}{r_{ab}}\right)^{12} - \left(\frac{\sigma_{ij}}{r_{ab}}\right)^{6}\right] + u_{\mathrm{Q}}(r_{ij}, \theta_i, \theta_j, \phi_{ij}, Q). \quad (1)$$

Here, r_{ab} is the distance between LJ site a and LJ site b; a counts the two sites of molecule i, and b counts those of molecule j. The LJ parameters σ_{ij} and ϵ_{ij} represent the size and energy parameters of the LJ potential, respectively. The quadrupolar contribution is given by [19]

$$u_{\mathrm{Q}}(r_{ij}, \theta_i, \theta_j, \phi_{ij}, Q) = \frac{3}{4}\frac{Q^2}{r_{ij}^5}[1 - 5(c_i^2 + c_j^2) - 15c_i^2c_j^2 + 2(s_is_jc - 4c_ic_j)^2], \quad (2)$$

with $c_k = \cos\theta_k$, $s_k = \sin\theta_k$, and $c = \cos\phi_{ij}$. Here, r_{ij} is the center–center distance of the two molecules i and j. θ_i is the angle between the axis of the molecule i and the center–center connection line, and ϕ_{ij} is the azimutal angle between the axis of molecules i and j. More details can be found in Gray and Gubbins [19].

Pure substance parameters were taken from Ref. 15 and are summarized in Table I. They were adjusted to experimental vapor pressure and saturated

liquid density data of the pure substance. For symmetric diatomic molecules fluorine (F_2) and nitrogen (N_2), and symmetric triatomic molecules like carbon dioxide (CO_2) and carbon disulfide (CS_2), as well as (C_2) derivates as ethane (C_2H_6) and ethylene (C_2H_4), the description of the interaction by the 2CLJQ represents a good approximation. However, since SF_6 molecules are neither elongated nor quadrupolar, the fitted parameters obtained for the 2CLJQ model lose all physical meaning.

For the modeling of mixtures, the like interactions are fully described by the pure substance models. The same holds for the unlike quadrupolar interaction, which is exactly determined by electrostatics, cf. Eq. (2). On the other hand, the parameters of the unlike LJ interactions are obtained from the pure fluid parameters by the modified Lorentz–Berthelot combination rule,

$$\sigma_{12} = \frac{(\sigma_{11} + \sigma_{22})}{2}, \tag{3}$$

and

$$\epsilon_{12} = \xi \cdot \sqrt{\epsilon_{11}\epsilon_{22}}, \tag{4}$$

where ξ is a binary interaction parameter that was adjusted to one experimental bubble point of the binary mixture. It has been shown in previous work of our group for numerous systems [20–22] that binary and ternary vapor–liquid equilibria can be described accurately in this way. The parameters used in this work were taken from Ref. 22, and their values are 1.041, 0.974, and 0.954 for $N_2 + CO_2$, $N_2 + C_2H_6$, and $CO_2 + C_2H_6$, respectively.

Table I. Potential Parameters for the Pure Fluids Used in This Work[a,b]

Fluid	σ (Å)	ϵ/k_B (K)	L (Å)	$10^{20}Q$ ($C \cdot m^2$)	M ($g \cdot mol^{-1}$)
F_2	2.8258	52.147	1.4129	2.9754	38.00
N_2	3.3211	34.897	1.0464	4.8024	28.01
CO_2	2.9847	133.22	2.4176	12.6549	44.01
CS_2	3.6140	257.68	2.6809	13.0081	76.14
C_2H_6	3.4896	136.99	2.3762	2.7609	30.07
C_2H_4	3.7607	76.950	1.2695	14.4468	28.05
C_2H_2	3.5742	79.890	1.2998	16.9218	28.05
SF_6	3.9615	118.98	2.6375	26.7074	146.06

[a] Values taken from Ref. 15.
[b] The molar mass M was taken from Ref. 27.

2.2. Diffusion Coefficients

Diffusion coefficients can be calculated by equilibrium molecular dynamics with the Green–Kubo formalism [23, 24]. In this formalism, transport coefficients are related to integrals of time-correlation functions of the corresponding fluxes. There are various methods to relate transport coefficients to time-correlation functions; a good review was given by Zwanzig [25]. The self-diffusion coefficient of a molecular fluid is characterized by the mass current of a single target molecule [26]. It is given by

$$D_i = \frac{1}{3N_i} \int_0^\infty dt \left\langle \sum_{k=1}^{N_i} \boldsymbol{v}_i^k(0) \cdot \boldsymbol{v}_i^k(t) \right\rangle, \tag{5}$$

where $\boldsymbol{v}_i^k(t)$ expresses the velocity vector of the center of mass of molecule k of species i, and $\langle \cdots \rangle$ denotes an ensemble average. Equation (5) yields the self-diffusion coefficient for component i by averaging over N_i molecules. Also, the expression for the binary MS diffusion coefficient $Đ_{12}$ is given in terms of velocities of the molecular the centers of mass

$$Đ_{12} = \frac{x_2}{3N_1} \left(\frac{x_1 M_1 + x_2 M_2}{x_2 M_2} \right)^2 \int_0^\infty \mathrm{d}t \left\langle \sum_{k=1}^{N_1} \boldsymbol{v}_1^k(0) \cdot \sum_{k=1}^{N_1} \boldsymbol{v}_1^k(t) \right\rangle, \tag{6}$$

where M_i denotes the molar mass and x_i is the mole fraction of species i.

The present simulations yield both self-diffusion coefficients and binary MS diffusion coefficients. Unfortunately, a direct comparison between the simulated and experimental binary MS diffusion coefficients is not possible for the investigated mixtures due to the absence of experimental data. Nevertheless, it is possible to estimate the binary MS diffusion coefficients from empirical equations that relate the self-diffusion coefficients or infinite dilution binary diffusion coefficients to the binary MS diffusion coefficients through simple functions of the composition. Here, three such equations are considered: Darken's equation [17], Caldwell and Babb's equation [16], and Vignes' equation [18]. Darken's equation relates the self-diffusion coefficients of both components D_1 and D_2 to the binary MS diffusion coefficient $Đ_{12}$,

$$Đ_{12} = D_1 x_2 + D_2 x_1. \tag{7}$$

It is important to note that the self-diffusion coefficients are needed for each studied composition so that Eq. (7) is only of limited use for practical aplications. Vignes' equation [18] and Caldwell and Babb's equation [16] relate the

MS diffusion coefficients to the infinite dilution binary diffusion coefficients D_{12}^{∞} and D_{21}^{∞}. The Caldwell and Babb equation is given by

$$Đ_{12} = D_{21}^{\infty} x_1 + D_{12}^{\infty} x_2, \tag{8}$$

and the Vignes equation by

$$Đ_{12} = (D_{21}^{\infty})^{x_1} (D_{12}^{\infty})^{x_2}. \tag{9}$$

Here, D_{ij}^{∞} is the diffusion coefficient of species i infinitely diluted in species j. In contrast to Darken's equation, the equations of Caldwell and Babb and of Vignes need only two values for the whole range of composition, which makes them attractive for practical applications. In the limit of infinite dilution, the binary MS diffusion coefficient and the self-diffusion coefficient coincide. This result can be obtained from Eq. (7), by taking the limit $x_i \to 0$, i.e., if $x_1 \to 0$ then $Đ_{12} = D_{12}^{\infty} = D_1$, or if $x_2 \to 0$ then $Đ_{21} = D_{21}^{\infty} = D_2$. This equivalence is used to obtain the self-diffusion coefficients in the infinite dilution limit.

2.3. Simulation Details

Molecular simulations were performed in a cubic box of volume V containing $N = 500$ molecules whose interactions are described by the 2CLJQ potential. The cut-off radius was set to $r_c = 5\sigma$ and the molecules were assumed to have no preferential relative orientations outside the cut-off sphere. For the calculation of the LJ long range corrections, orientational averaging was applied with equally weighted relative orientations as proposed by Lustig [28]. The assumption of no preferential relative orientations beyond the cut-off sphere implies for the quadrupolar interactions that long range corrections are not needed since they vanish. The simulations were started from a face-centered-cubic lattice configuration with randomly distributed velocities, the total momentum of the system was set to zero, and modified Newton's equations of motion were solved with the Gear predictor-corrector integration scheme of fifth order [29]. The time step for this algorithm was set to $\Delta t \sqrt{\epsilon_1 / m_1} / \sigma_1 = 0.001$. The time-correlation functions were calculated in the NVT ensemble using the Nosé-Hoover thermostat [30, 31] with a thermal inertial parameter of $10\,\mathrm{kJ \cdot mol^{-1} \cdot ps^2}$, and the diffusion coefficients were then obtained by using Eqs. (5) and (6).

It must be pointed out that both NVE and NVT simulations were performed, and the obtained diffusion coefficients agreed in all cases

within their uncertainties. It was concluded that the Nosé–Hoover thermostat does not influence the values of the diffusion coefficients. As NVT simulations yield diffusion coefficients exactly at the desired temperature, they were preferred. The simulations were equilibrated in a NVT ensemble over 100,000–150,000 time steps. Once equilibrium has been reached, the self-diffusion and MS diffusion coefficients were evaluated. To calculate the binary MS diffusion coefficients at the desired T and p, a prior NpT simulation [32] was performed, from which the density for the NVT ensemble was taken. The statistical uncertainty of the diffusion coefficients was estimated using the method of Fincham et al. [33]. In order to calculate the self-diffusion and binary diffusion coefficients, similar criteria as in Ref. 8 were applied. Self-diffusion coefficients were calculated by averaging over 100,000 independent autocorrelation functions, i.e., over 200 time origins. The time origins were taken every 500th time step during the period of production. Depending on the density, this distance between time origins was extended in order to ensure their independence. The correlation function was calculated over 2500 time steps in order to minimize the error due to the long-time tail. From pilot runs with different lengths of correlations functions, i.e., 1000, 2500, and 3500 time steps, this error was estimated to be about 3%. For the calculation of the binary MS diffusion coefficients, 12,000 independent time origins were averaged, here a compromise between accuracy and simulation time was made. The time origins were taken every 100th time step, and the correlation function was calculated over 1000–1500 time steps. This requires simulations of about 1×10^5 to 4×10^5 time steps for the self-diffusion coefficients and 12×10^5 for MS diffusion coefficients. The binary MS diffusion coefficients were calculated for mole fractions between 0.1 and 0.9. To obtain the binary MS diffusion coefficients at infinite dilution, a polynomial function was fitted to the simulation results between mole fractions 0.1 and 0.9 and then extrapolated to zero and one, respectively. The relative error was estimated as being the same as for the binary MS diffusion coefficients at 0.1 and 0.9, respectively.

An important issue is the influence of the moments of inertia of the molecules on the self-diffusion coefficient. In all cases, the experimental molecular mass [27] was distributed equally between the two LJ centers. However, for CO_2 this matter was investigated. For CO_2, the experimental molecular mass was distributed between the two LJ centers and the quadrupolar site, so that the mass of the two oxygen atoms was distributed between the two LJ centers, and the mass of the carbon atom was associated with the quadrupolar site. In this case, the tensor of moments of inertia in a reference system with origin in the geometrical center of the CO_2 molecule is diagonal, whose two nonzero elements are given by

$4000\,L^2 \cdot \mathrm{g} \cdot \mathrm{mol}^{-1} \cdot \mathrm{m}^2$. On the other hand, if the moment of inertia is calculated sharing the total molecular mass between the two LJ centers only, the diagonal elements have a value of $5501\,L^2 \cdot \mathrm{g} \cdot \mathrm{mol}^{-1} \cdot \mathrm{m}^2$. No difference for the self-diffusion coefficients was found for the two different choices. This result is plausible, because the self-diffusion coefficient is related to the translational motion of the molecular center of mass.

3. RESULTS

In this section, the predictions for self- and binary MS diffusion coefficients are compared to experimental data and to the empirical equation of Liu et al. [34], which is a correlation based on molecular simulation results and experimental data. The results are presented in terms of the product of self-diffusion coefficient and density rather than the self-diffusion coefficient itself, because the latter tends to infinity in the zero density limit. The self-diffusion coefficient is a single-particle property, thus highly accurate data can be obtained with modest computing time. The uncertainty of the present self-diffusion data is less than 1%; numerical values for all fluids are given in Table II.

3.1. Self-Diffusion Coefficients in Pure Fluids

Figure 1 shows the results for the product of density and self-diffusion coefficient of F_2, N_2, CO_2, and CS_2 compared to experimental data [35–38]. For F_2 and N_2, the considered state points correspond to the saturated liquid, for which experimental densities were taken from Refs. 39 and 40. For CO_2 and CS_2, the state points lie in the homogeneous liquid region at temperatures of 273 and 298.2 K, respectively. Overall, fair agreement between experimental data and the predictions by molecular simulation is found. The best results are obtained for N_2 with an average deviation of only 6%. For F_2, the predictions match the experimental data at high densities, at low densities deviations up to 20% occur. The predictions for CO_2 are too low by about 20%. For CS_2, the predictions are also too low by about the same amount; in this case the correlation of Liu shows better agreement with the experimental data. It should be noted that the poorer performance of the CO_2 and CS_2 models is reasonable since the three atoms of roughly the same size have not been explicitly considered by the 2CLJQ model.

Figure 2 shows the results for the product of density and self-diffusion coefficient of C_2H_6, C_2H_4, C_2H_2, and SF_6 compared to experimental data [41–44] and Liu's correlation. For C_2H_6 and C_2H_4 the considered state points lie in the homogeneous liquid region at temperatures of 273 and

Table II. Self-diffusion Coefficients for F_2, N_2, CO_2, CS_2, C_2H_6, C_2H_4, C_2H_2, and SF_6 Predicted by Molecular Simulation Compared to Experimental Data

T (K)	$10^{-3}\rho$ (mol·m^{-3})	$10^9 D^{exp.}$ (m^2·s^{-1})	$10^9 D^{sim.}$ (m^2·s^{-1})	T (K)	$10^{-3}\rho$ (mol·m^{-3})	$10^9 D^{exp.}$ (m^2·s^{-1})	$10^9 D^{sim.}$ (m^2·s^{-1})
F_2				N_2			
54.0	44.824	0.569	0.569(2)	77.0	28.861	2.526	2.923(8)
62.0	43.497	1.05	0.905(2)	80.0	28.380	2.996	3.309(5)
70.0	42.166	1.69	1.361(3)	83.0	27.870	3.509	3.757(8)
78.0	40.787	2.46	1.903(6)	85.0	27.526	3.875	4.03(1)
88.0	38.968	3.57	2.793(8)	88.0	27.006	4.459	4.63(1)
96.0	37.405	4.55	3.575(6)	90.0	26.643	4.871	4.93(1)
105.0	35.497	5.73	4.74(1)	93.0	26.079	5.522	5.54(1)
CO_2				C_2H_4			
273.0	21.102	13.50	10.41(3)	298.15	4.4955	113.6	110.0(3)
273.0	21.453	13.00	10.39(6)	298.15	6.2923	79.91	76.1(3)
273.0	22.333	11.70	9.274(3)	298.15	8.0927	62.10	56.6(1)
273.0	23.046	10.70	8.156(4)	298.15	9.8895	49.45	42.1(2)
273.0	23.460	10.00	7.890(2)	298.15	11.690	39.58	33.20(8)
273.0	23.900	9.50	7.518(4)	298.15	13.487	31.21	25.5(1)
				298.15	15.283	24.08	19.90(7)
				298.15	17.084	18.20	14.60(3)
				298.15	18.881	13.44	10.70(3)
				298.15	20.681	9.927	7.28(9)
C_2H_6				CS_2			
273.0	15.431	14.6	14.40(4)	298.2	16.489	4.26	3.209(7)
273.0	16.550	11.8	11.71(6)	298.2	17.019	3.64	2.653(8)
273.0	17.968	8.91	9.008(4)	298.2	17.514	3.21	2.264(7)
273.0	18.902	7.24	7.230(2)	298.2	18.031	2.61	1.867(5)
273.0	19.609	6.27	5.870(1)	298.2	18.543	2.23	1.532(5)
C_2H_2				SF_6			
192.0	23.754	3.74	2.91(1)	240.0	12.091	3.35	3.52(3)
197.0	23.463	4.26	3.37(1)	250.0	11.653	3.94	4.28(2)
202.0	23.167	4.82	3.95(1)	260.0	11.221	4.66	4.89(4)
207.0	22.863	5.43	4.35(1)	270.0	10.742	5.59	6.03(2)
212.0	22.554	6.07	4.66(1)	280.0	10.201	6.71	7.49(4)
217.0	22.237	6.76	5.44(1)	290.0	9.606	8.29	8.87(5)
222.0	21.912	7.49	5.95(2)	300.0	8.846	10.5	11.00(2)
310.0	7.826	14.4	14.50(5)				

298.15 K, respectively. For C_2H_2 and SF_6 the states correspond to the saturated liquid; the C_2H_2 densities were taken from Ref. 45. Good agreement with the experimental data is found. The best results are found for C_2H_6 and SF_6, with average deviations of only 2 and 6%. For C_2H_2, the predictions of

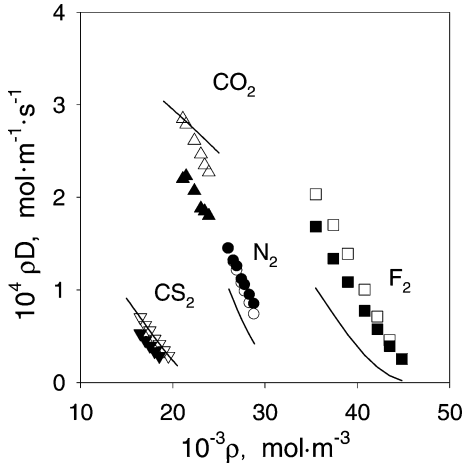

Fig. 1. Self-diffusion coefficients of fluorine, nitrogen, carbon dioxide, and carbon disulfide as predicted by molecular simulation in comparison to experimental data [35–38]. F_2 (saturated liquid, $T = 54 - 105$ K): □ exp., ■ sim.; N_2 (saturated liquid, $T = 77 - 93$ K): ○ exp., ● sim.; CO_2 (homogeneous liquid, $T = 273$ K): △ exp., ▲ sim.; CS_2 (homogeneous liquid, $T = 298.2$ K): ▽ exp., ▼ sim. The lines represent the correlation of Liu et al. [34].

the simulation are too low by about 20%; for C_2H_4, they are also too low by about 15%. The experimental data of C_2H_4 show a pronounced curvature that is neither reproduced by the simulations nor by Liu's correlation. Liu's correlation is as good as the simulation for SF_6 and C_2H_6, worse than the simulation for C_2H_2, but slightly better for C_2H_4.

To study the dependence of the self-diffusion coefficient on the number of particles, one state point for N_2 at $T = 85$ K, $\rho = 27.526 \times 10^3$ mol · m^{-3} was chosen. For this state point, a sequence of simulations with increasing number of particles: $N = 108$, 256, 500, 864, and 1372 was carried out. The values for the self-diffusion coefficients were 3.78(6), 3.96(5), 4.03(1), 4.13(2), 4.21(2) in 10^{-9}m^2· s^{-1}, respectively. An estimate of the self-diffusion coefficient for an infinite system size can be obtained by a linear fit of the self-diffusion coefficient data as a function of the inverse box length [46]. This fit yields a value of $4.50(4) \times 10^{-9}$ m^2· s^{-1} for an infinitely large system, that is about 10% larger than the results with $N = 500$ particles. As most predictions of self-diffusion coefficients are below the experimental data, the finite-size correction can improve the

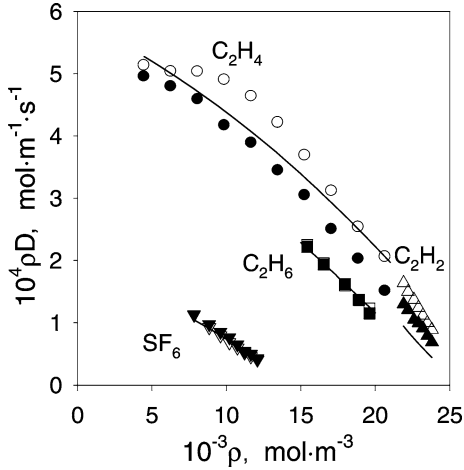

Fig. 2. Self-diffusion coefficients of ethane, ethylene, acetylene, and sulfur hexafluoride as predicted by molecular simulation in comparison to experimental data [38, 41–43]. C_2H_6 (homogeneous liquid, $T = 273$ K): □ exp., ■ sim.; C_2H_4 (homogeneous liquid, $T = 298.15$ K): ○ exp., ● sim.; C_2H_2 (saturated liquid, $T = 192 - 222$ K): △ exp., ▲ sim.; SF_6 (saturated liquid, $T = 240 - 310$ K): ▽ exp., ▼ sim. The lines represent the correlation of Liu et al. [34].

agreement with the experimental data for most fluids. Exceptions are F_2, SF_6, and C_2H_6, for which the deviations would increase.

3.2. Binary Maxwell–Stefan Diffusion Coefficients

In this section, the results obtained for the binary mixtures N_2+CO_2, N_2+C_2H_6, and CO_2+C_2H_6 at 253.15 K and 20 MPa are presented. Numerical data are given in Table III: self-diffusion coefficients of pure fluids in binary mixtures are reported with statistical uncertainties less than 1%; and binary MS diffusion coefficients are reported with statistical uncertainties of about 10%. These mixtures were selected since their vapor–liquid equilibria were successfully calculated with the present molecular models [22]. The simulated MS diffusion coefficients are compared with the predictions from the equations of Darken, Caldwell and Babb, and Vignes, cf. Eqs. (7)–(9). To evaluate their performance, the average relative deviation, $\sum_i (Đ_{12,i}^{\text{sim}} - Đ_{12,i}^{\text{equation}})/Đ_{12,i}^{\text{sim}}$, was calculated. Experimental data for comparison are unfortunately not available. The input needed for Eqs.

Table III. Self-diffusion and Binary MS Diffusion Coefficients of the Binary Mixtures $N_2 + CO_2$, $N_2 + C_2H_6$, and $CO_2 + C_2H_6$ at 253.15 K and 20 MPa Predicted by Molecular Simulation

x_1	$10^{-3}\rho$ (mol·m^{-3})	$10^9 D_1$ (m^2·s^{-1})	$10^9 D_2$ (m^2·s^{-1})	$10^9 Đ_{12}$ (m^2·s^{-1})
$N_2(1) + CO_2(2)$				
0.0	24.08	8.7(9)	6.86(2)	8.7(9)
0.1	22.96	11.57(7)	8.40(3)	11.7(5)
0.2	21.47	14.60(7)	10.55(4)	15.4(3)
0.4	17.73	24.13(10)	16.74(2)	26(1)
0.5	15.59	30.77(8)	21.19(7)	31(1)
0.6	13.60	38.63(6)	26.83(19)	37(2)
0.8	10.90	53.87(20)	38.39(25)	47(3)
0.9	9.968	61.25(20)	44.08(24)	46(3)
1.0	9.356	67.49(13)	43(4)	43(4)
$N_2(1) + C_2H_6(2)$				
0.0	13.87	20(1)	11.97(4)	20(1)
0.1	13.85	17.39(9)	13.27(2)	18(1)
0.2	13.74	19.58(16)	14.98(4)	18(1)
0.4	12.91	26.48(6)	19.81(11)	26(2)
0.6	11.21	42.88(50)	31.18(20)	39(3)
0.8	9.302	54.42(11)	40.25(38)	48(4)
0.9	8.566	62.88(17)	47.08(40)	48(4)
1.0	8.059	70.21(20)	47(4)	47(4)
$CO_2(1) + C_2H_6(2)$				
0.0	16.10	13(1)	11.84(1)	13(1)
0.1	16.47	12.38(14)	11.75(6)	13(1)
0.2	16.88	11.98(5)	11.64(6)	13(1)
0.4	17.95	10.93(6)	11.09(8)	13(1)
0.6	19.49	9.63(4)	10.08(6)	12(1)
0.8	21.59	8.09(3)	8.66(9)	10.3(8)
0.9	22.94	7.21(1)	7.78(14)	8.2(7)
1.0	24.66	6.15(6)	5.1(7)	5.1(7)

(7)–(9) were therefore simulation data, i.e., self-diffusion coefficients for Darken's equation and infinite dilution diffusion coefficients for the equations of Caldwell and Babb and of Vignes.

Figure 3 shows the results for the binary MS diffusion coefficients for the mixture $N_2 + CO_2$ compared to the equations of Caldwell and Babb, Darken, and Vignes. The MS diffusion coefficient increases as the mole fraction of N_2 increases due to the smaller size and mass of the N_2 molecule. The simulation results lie above the linear interpolation between the infinite dilution diffusion coefficients, i.e., Caldwell and Babb's equation. Vignes' equation gives a different behavior, with negative deviations from

the linear interpolation, whereas Darken's equation predicts positive deviations from the linear interpolation for high N_2 mole fractions and negative deviations for low mole fractions.

Figure 4 shows the results for the binary MS diffusion coefficients of the mixture $N_2 + C_2H_6$. In this case, the MS diffusion coefficients lie below the linear interpolation of the infinite dilution diffusion coefficients for mole fractions smaller than 0.5 and lie above the linear interpolation for mole fractions larger than 0.5. The results of Darken's equation agree well with the simulation data. The average deviation is only about 6%. The equation of Vignes fails to reproduce the shape of the curve, which results in an average deviation of about 20%. The deviations between the simulation results and the correlation of Caldwell and Babb are also about 20%.

Figure 5 shows the results for the binary MS diffusion coefficients of the mixture $CO_2 + C_2H_6$. In this case, the MS diffusion coefficients lie above the linear interpolation between the infinite dilution diffusion coefficients (Caldwell and Babb) over the whole composition range. Also, Darken's equation here yields the best results, with an average deviation of 12%, whereas the equations of Caldwell and Babb and of Vignes yield deviations of 23% and 28%, respectively. Again Vignes' equation does not reproduce the sign of the deviations from the linear interpolation correctly.

Figures 3–5 show that the curvature of the MS diffusion coefficient is a function of the mole fraction, depending qualitatively on the mixture. It

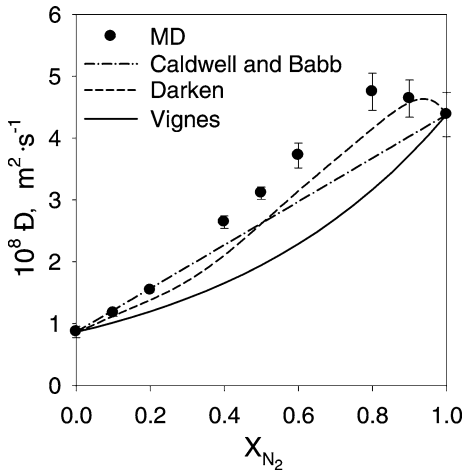

Fig. 3. Binary MS diffusion coefficients for the mixture $N_2 + CO_2$ at 253.15 K and 20 MPa as predicted by molecular simulation in comparison to empirical equations.

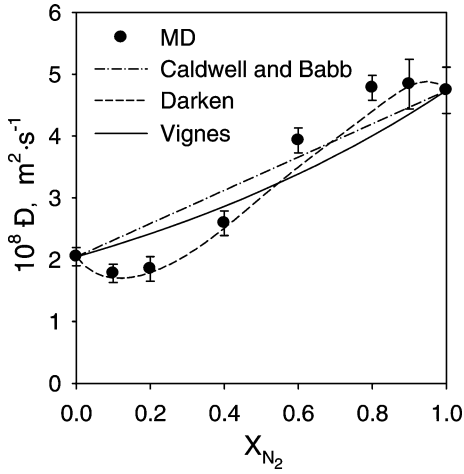

Fig. 4. Binary MS diffusion coefficients for the mixture N_2+C_2H_6 at 253.15 K and 20 MPa as predicted by molecular simulation in comparison to empirical equations.

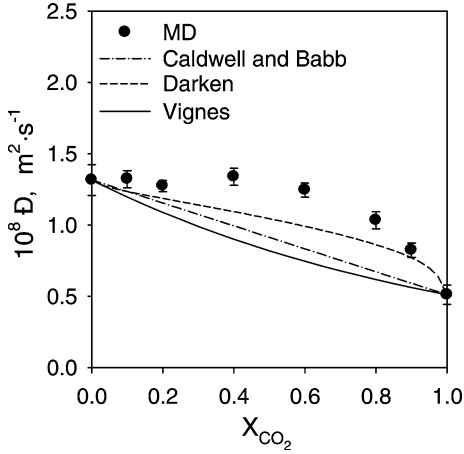

Fig. 5. Binary MS diffusion coefficients for the mixture CO_2+C_2H_6 at 253.15 K and 20 MPa as predicted by molecular simulation in comparison to empirical equations.

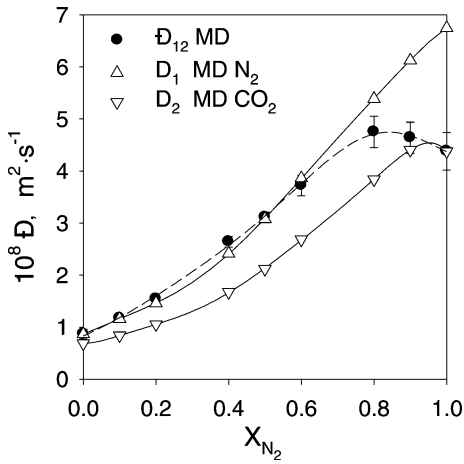

Fig. 6. Self- and binary MS diffusion coefficients for the mixture $N_2(1)+CO_2(2)$ at 253.15 K and 20 MPa as predicted by molecular simulation: $\triangle D_1$; $\triangledown D_2$; $\bullet Đ_{12}$. The lines serve as guide for the eye.

can be concave, with a positive deviation from the linear course, or convex with a negative deviation, or both. The investigated mixtures are not strongly polar, and also in the 2CLJQ models only quadrupolar interactions are present. However, the MS diffusion coefficients of these mixtures cannot be well represented by the equations of Caldwell and Babb or of Vignes, which are often claimed to be adequate for such simple mixtures [18].

Dullien [47] compared the predictions of Vignes' equation with experimental data, and also found that in many cases, where the mixtures were nonassociating, the equation of Vignes was not able to predict the binary MS diffusion coefficients correctly. The equation of Darken shows the best performance in all cases. That is due to the fact that it uses more information than the other two. Moreover, it can be shown that it is exact if the cross correlations between different particles of the same species and particles of different species are neglected [5]. Unfortunately, Darken's equation is of little use for most practical applications.

3.3. Binary Self-diffusion Coefficients

Figures 6–8 show the results for self-diffusion coefficients of the pure components in the mixtures $N_2 + CO_2$, $N_2 + C_2H_6$, and $CO_2 + C_2H_6$ at

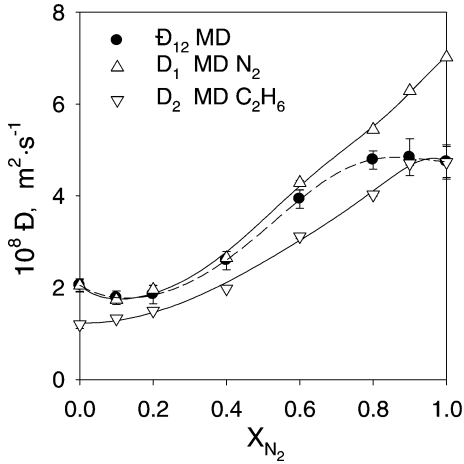

Fig. 7. Self- and binary MS diffusion coefficients for the mixture $N_2(1)+C_2H_6(2)$ at 253.15 K and 20 MPa as predicted by molecular simulation: $\triangle D_1; \triangledown D_2; \bullet Đ_{12}$. The lines serve as guide for the eye.

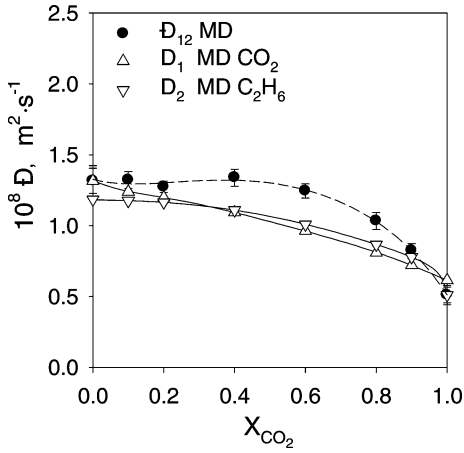

Fig. 8. Self- and binary MS diffusion coefficients for the mixture $CO_2(1)+C_2H_6(2)$ at 253.15 K and 20 MPa as predicted by molecular simulation: $\triangle D_1; \triangledown D_2; \bullet Đ_{12}$. The lines serve as guide for the eye.

253.15 K and 20 MPa, together with those for the binary MS diffusion coefficients. For $N_2 + CO_2$ and $N_2 + C_2H_6$, the MS diffusion coefficients can qualitatively be described by a simple interpolation as indicated by Darken's equation. The situation is different for $CO_2+C_2H_6$, cf. Fig. 8. The self-diffusion coefficients are almost equal for that mixture at all compositions. Nevertheless, the MS diffusion coefficient from the simulations is larger, so that Eq. (7) is inappropriate.

4. CONCLUSION

In the present work, molecular dynamics simulation and the Green–Kubo formalism were used to calculate self- and binary MS diffusion coefficients for a class of fluids modeled by the 2CLJQ intermolecular potential. The potential parameters were taken from previous work [15, 22], where they were adjusted to experimental vapor–liquid equilibria only. Eight pure fluids, i.e., F_2, N_2, CO_2, CS_2, C_2H_6, C_2H_4, and C_2H_2 and three binary mixtures, i.e., N_2+CO_2, $N_2+C_2H_6$, and $CO_2+C_2H_6$, were studied. Self-diffusion coefficients are reported with statistical uncertainties smaller than 1%. These results do not consider corrections due to the long-time tail; the error due to it is estimated to be about 3%. Deviations between the predicted and the experimental data do not exceed 20%. The correction due to the finite size of the simulated system increases the self-diffusion coefficients typically by 10%. With this correction, an even better agreement can be expected for most fluids. Exceptions are F_2, SF_6, and C_2H_6 for which the deviations would increase.

For the binary mixtures, predictions from the simulations are only compared to results from the equations of Darken, Caldwell and Babb, and Vignes, as experimental data were not available. The self-diffusion coefficients are reported with statistical uncertainties smaller than 1%, and the binary MS diffusion coefficients are reported with statistical uncertainties of about 10%. In agreement with previous findings [8], Darken's equation yields the best agreement in all cases with average deviations of only 10%. Unfortunately, this equation requires self-diffusion coefficients in the mixture as input data. The two simple equations of Caldwell and Babb and of Vignes which use infinite dilution diffusion coefficients as input data, fail to predict the shape of the composition dependence of the MS diffusion coefficients, which shows a strong curvature, despite the fairly simple molecules studied here. This indicates that more accurate correlations for the prediction of MS diffusion coefficients are needed. For their development, molecular simulation is a useful tool, as it can relate molecular properties, i.e., polarity, anisotropy etc. to diffusion coefficients.

REFERENCES

1. B. J. Alder and T. E. Wainwright, *Phys. Rev. Lett.* **18**:988 (1967).
2. B. J. Alder and T. E. Wainwright, *Phys. Rev. A* **1**:18 (1970).
3. G. Jaccuci and I. R. McDonald, *Physica A* **80**:607 (1975).
4. D. Jolly and R. Bearman, *Mol. Phys.* **41**:137 (1980).
5. M. Schoen and C. Hoheisel, *Mol. Phys.* **52**:33 (1984).
6. J. M. Stoker and R. L. Rowley, *J. Chem. Phys.* **91**:3670 (1989).
7. R. L. Rowley and J. M. Stoker, *Int. J. Thermophys.* **12**:501 (1991).
8. G. A. Fernández, J. Vrabec, and H. Hasse, *Int. J. Thermophys.* **25**:175 (2004).
9. G. A. Fernández, J. Vrabec, and H. Hasse, *Fluid Phase Equilib.* **221**:157 (2004).
10. I. R. McDonald and K. Singer, *Mol. Phys.* **23**:29 (1972).
11. P. S. Y. Cheung and J. G. Powles, *Mol. Phys.* **30**:921 (1975).
12. R. Vogelsang and C. Hoheisel, *Phys. Chem. Liq.* **16**:189 (1987).
13. C. Hoheisel, *Mol. Phys.* **62**:239 (1987).
14. D. Möller and J. Fischer, *Fluid Phase Equilib.* **100**:35 (1994).
15. J. Vrabec, J. Stoll, and H. Hasse, *J. Phys. Chem. B* **105**:12126 (2001).
16. C. S. Caldwell and A. L. Babb, *J. Phys. Chem.* **60**:51 (1956).
17. L. S. Darken, *Trans. Am. Inst. Mining Metall. Eng.* **175**:184 (1948).
18. A. Vignes, *Ind. Eng. Chem. Fundam.* **5**:189 (1966).
19. C. G. Gray and K. E. Gubbins, *Theory of Molecular Fluids*, *Vol. 1: Fundamentals*, (Clarendon Press, Oxford, 1984).
20. J. Vrabec and J. Fischer, *AIChE J.* **43**:212 (1996).
21. J. Vrabec, J. Stoll, and H. Hasse, *Mol. Sim.* **31**:215 (2005).
22. J. Stoll, J. Vrabec, and H. Hasse, *AIChE J.* **49**:2187 (2003).
23. M. S. Green, *J. Chem. Phys.* **22**:398 (1954).
24. R. Kubo, *J. Phys. Soc. Japan* **12**:570 (1957).
25. R. Zwanzig, *Ann. Rev. Phys. Chem.* **16**:67 (1965).
26. C. Hoheisel, *Phys. Rep.* **245**:111 (1994).
27. NIST Chemistry WebBook, http://webbook.nist.gov/chemistry.
28. R. Lustig, *Mol. Phys.* **65**:175 (1988).
29. J. M. Haile, *Molecular Dynamics Simulation* (John Wiley & Sons., New York, 1997).
30. S. Nosé, *Mol. Phys.* **100**:191 (2002).
31. D. Frenkel and B. Smit, *Understanding Molecular Simulation* (Academic Press, San Diego, 1996).
32. H. C. Andersen, *J. Chem. Phys.* **72**:2384 (1980).
33. D. Fincham, N. Quirke, and D. J. Tildesley, *J. Chem. Phys.* **84**:4535 (1986).
34. H. Liu, C. M. Silva, and E. A. Macedo, *Chem. Eng. Sci.* **53**:2403 (1998).
35. D. E. O'Reilly, E. M. Peterson, D. I. Hogenboom, and C. E. Scheie, *J. Chem. Phys.* **54**:4194 (1971).
36. K. Krynicki, E. J. Rahkamaa, and J. P. Powles, *Mol. Phys.* **28**:853 (1974).
37. P. E. Etesse, J. A. Zega, and R. Kobayashi, *J. Chem. Phys.* **97**:2022 (1992).
38. L. A. Woolf, *J. Chem. Soc. Faraday Trans. 1* **78**:583 (1982).
39. N. B. Vargaftik, Y. K. Vinogradov, and V. S. Yargin, *Handbook of Physical Properties of Liquids and Gases* (Begell House, New York, 1996).
40. E. W. Lemmon, M. O. McLinden, and M. L. Huber, *REFPROP* (NIST Standard Reference Database 23, Version 7.0, 2002).
41. A. Greiner-Schmid, S. Wappmann, M. Has, and H. D. Lüdemann, *J. Chem. Phys.* **94**:5643 (1991).
42. B. Arends, K. O. Prins, and N. J. Trappeniers, *Physica A* **107A**:307 (1981).

43. C. E. Scheie, E. M. Peterson, and D. E. O'Reilly, *J. Chem. Phys.* **59**:2303 (1973).
44. J. K. Tison and E. R. Hunt, *J. Chem. Phys.* **54**:1526 (1971).
45. T. E. Daubert and R. P. Danner, *Data Compilation Tables of Properties of Pure Substances*, AIChE (American Chemical Society, New York, 1985).
46. I. Yeh and G. Hammer, *J. Chem. Phys.* **108**:158 (2004).
47. F. A. L. Dullien, *Ind. Eng. Chem. Fundam.* **10**:41 (1971).